Geomechanics and Engineering, *Vol. 18, No. 2 (2019) 121-131*
DOI: https://doi.org/10.12989/gae.2019.18.2.121

Compression and shear responses of structured clays during subyielding

Jirayut Suebsuk*[1], Suksun Horpibulsuk[2a] and Martin D. Liu[3b]

[1]*Department of Civil Engineering, Faculty of Engineering and Architecture, Rajamangala University of Technology Isan, Nakhon Ratchasima, Thailand*
[2]*School of Civil Engineering and Center of Excellence in Innovation for Sustainable Infrastructure Development, Suranaree University of Technology, Nakhon Ratchasima, Thailand*
[3]*Faculty of Engineering, The University of Wollongong, New South Wales, Australia*

(Received September 15, 2017, Revised May 12, 2019, Accepted May 13, 2019)

Abstract. This article discusses the phenomenon of plastic volumetric deformation of naturally structured clays before virgin yielding, i.e., subyielding behavior. A simple approach representing both the compression and shear responses of the clays during subyielding is demonstrated. A new compression model for structured clays based on the theoretical framework of the Structured Cam Clay (SCC) model via incorporation of the subyielding behavior is presented. Two stress surfaces are introduced to distinguish the subyielding and virgin yielding. The hardening and destructuring processes of structured clays under isotropic compression and shear are the focus of this work. The simulations of the compression and shear of eleven natural clays are studied for validation. The proposed work can accurately predict the subyielding behavior of structured clays both qualitatively and quantitatively and can be used for modeling structured clays under compression and shear responses in geological and geotechnical engineering problems.

Keywords: hardening; destructuring; structured cam clay; structured clay; subyielding

1. Introduction

Compression and shear responses are two essential parts of soil deformation. Modeling or predicting the deformation of geomaterials is necessary to solve geological and geotechnical engineering problems (e.g., Chai *et al.* 2004, Herbstová and Herle 2009, Gyllanda *et al.* 2013). Clays in situ usually possess natural structures. After deposition, the clay sediments may undergo various diagenesis changes. The stress to which the soil has been subjected, the environments during and after deposition, and time are known as potential factors for development of soil structure. Many researchers have reported the development of soil structure during deposition and postdepositional processes (e.g., Locat and Lefebvre 1985, Schmertmann 1991). In this study, the term "soil structure" refers to the fabric (particle associations and arrangements) and to the soil cementation (bonding or interparticle forces) (e.g., Leroueil and Vaughan 1990). Recent studies have revealed that the mechanical behavior of structured and reconstituted clays are different (e.g., Burland 1990, Carter *et al.* 2000, Cotecchia and Chandler 2000, Horpibulsuk *et al.* 2007, Leroueil and Vaughan 1990, Park 2016).

The critical state soil mechanics has been widely used for modeling the deformation of clay deposits (Schofield and Wroth 1968). There is much research on the constitutive model of clay (e.g., Roscoe and Schofield 1963, Roscoe and Burland 1968, Yao *et al.* 2008, 2009, Shen and Xu 2011, Shen *et al.* 2013, Yao and Zhou 2013). The Cam Clay model successfully describes the behavior of reconstituted clay without considering soil structure (Roscoe and Schofield 1963; Roscoe and Burland 1968). Since then, there has been much progress in modeling natural clay behavior with due consideration of soil structure. Some of this work has been presented by Gen and Nova (1993), Baudet and Stallebrass (2004), Gajo and Muir Wood (2001), Kavvadas and Amorosi (2000), Rouainia and Muir Wood (2000), Chen *et al.* (2014), Zhu and Yao (2015), Ouria (2017), Zhang *et al.* (2017). The effect of soil structure has been taken into account in an extended version of the Cam Clay model by Liu and Carter; e.g., the 'Structured Cam Clay' (SCC) model (Liu and Carter 2002, Carter and Liu 2005). The SCC model was formulated based on a study of the virgin (structured) compression line (Liu and Carter 1999; and Liu and Carter 2000). The state parameter for the identification of the effect of soil structure on volumetric deformation is the different void ratios between the structured compression line (SCL) and the intrinsic (reconstituted) compression line (ICL). The structure and destructuring laws were implicated according to the volumetric hardening and softening model formulation. In the SCC model, the purely elastic behavior (e.g., the preyield state) and elastoplastic behavior (e.g., the yielding state) are separated by a yield surface. However, nonrecoverable behavior upon unloading and repeated loading have been observed for loading before the yielding of clays and many other geomaterials (e.g., Burland 1990,

*Corresponding author, Assistant Professor
E-mail jirayut.su@rmuti.ac.th
[a]Professor
E-mail: suksun@g.sut.ac.th
[b]Senior Lecturer
E-mail: martindl@uow.edu.au

http://www.techno-press.org/?journal=gae&subpage=7
ISSN: 2005-307X (Print), 2092-6219 (Online)

Leroueil and Vaughan 1990, Carter *et al.* 2000, Callisto and Rampello 2004, Sun *et al.* 2015, Cheng and Wang 2016). The SCC model consequently underestimates the deformation of the soil before virgin yielding. A nonsmooth continuity between pre- and postyielding of soil during compression and shear is a shortcoming of the conventional plasticity model. It is necessary to capture soil behaviors for stress excursions inside the yield surface for a reliable prediction of soil response before virgin yielding.

Liu and Carter (2003) proposed the subyielding concept for modeling soil in the preyielding state. The soil was modeled as a subyielding material before virgin yielding. Plastic deformation during subyielding is generally induced by a stress change inside the yield surface, as well as by a stress change originating on the current yield (loading) surface causing it to expand. The variation of the loading surface is modeled with plastic volumetric deformation considering destructuring as well as hardening. The yield surface expands and is coincident with the loading surface during virgin yielding. The subyielding concept can solve the limitations of the conventional plasticity model for modeling the behavior of soil before virgin yielding.

This research article presents a practical (simple and rational) model for volumetric deformation of structured soils under compression and shear responses based on the subyielding concept. A compression equation for subyielding behavior of structured clays is proposed. The corresponding equations describing the hardening and destructuring is also presented, implicitly employing the plastic volumetric deformation as a state parameter. The formulation of the subyielding surface and its equations are extended to predict the undrained stress path of structured clays during shear. Simulations of both the compression and shear responses of eleven natural clays are made. A discussion of the model performance and the modeling of structured clays, in general, is also provided.

2. Compression behavior of structured clays

As a consequence of soil structure, the void ratio sustained by the structured clay is higher than that of the reconstituted clay. The additional void ratio sustained by the soil cementation structure decreases after virgin yielding. The breaking down of the soil structure occurs. With the breakdown of soil structure in virgin yielding, the SCL of structured clay is asymptotic to the ICL of reconstituted clay. Thus, Liu and Carter (1999) used the ICL as a reference for modeling the compression curves of structured clays. Based on the examination of experimental data, the compression model of structured soils was proposed by Liu and Carter (2000, 2002), as shown in Fig. 1. A general compression equation for the isotropic virgin compression of clays was also proposed

$$e = e^* + \Delta e = \left(e^*_{IC} - \lambda^* \ln p'\right) + \Delta e_i \left(\frac{p'_{y,i}}{p'}\right)^b \tag{1}$$

The definition of parameters Δe, Δe_i, $p'_{y,i}$, and b is presented in Fig. 1. e is the void ratio of structured soil and e^* is the void ratio of the same soil in a reconstituted state.

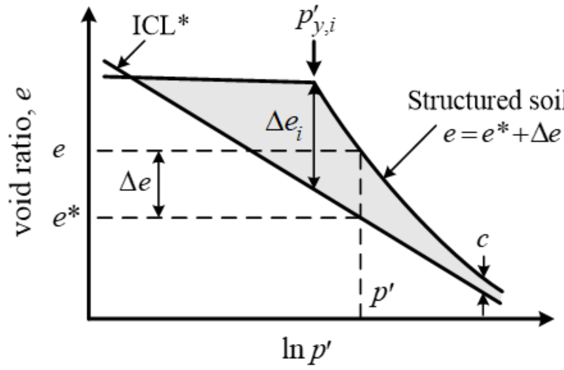

Fig. 1 Compression model of structured clay after Liu and Cater (2000, 2002)

Δe is the additional void ratio, which is the difference in the void ratio between a structured soil and the corresponding reconstituted soil at the same stress state. $p'_{y,i}$ is the mean effective stress (p') at which virgin yielding of the structured soil begins. Thus Δe_i is the additional void ratio at $p' = p'_{y,i}$. b is the rate of destructuring during virgin yielding (termed as the destructuring index). c is the additional void ratio sustained by a soil structure that cannot be eliminated by an increase in stress (Liu *et al.* 2006). For naturally structured soils, c is assumed to diminish when $p' \to \infty$. λ^* is the gradient of the ICL.

Based on the proposed work by Liu and Carter (2000; 2002), a compression equation for structured soils with volumetric hardening and destructuring for loading along the general stress path can be obtained as follows

$$e = e^*_{IC} - \kappa^* \ln p' + \Delta e_i \left(\frac{p'_{y,i}}{p'_s}\right)^b - \left(\lambda^* - \kappa^*\right) \ln p'_s \tag{2}$$

where e^*_{IC} is the void ratio at a reference mean effective stress (1 kPa) of the ICL and κ^* is the gradient of the recompression line. p'_s is a reference size of structural yield surface (stress history). Differentiating Eq. (2), the following incremental form for the volumetric deformation of structured soils during virgin yielding is obtained as follows

$$d\varepsilon_v = \frac{\kappa^*}{1+e}\left(\frac{dp'}{p'}\right) + \left[(\lambda^* - \kappa^*) + b\langle \Delta e \rangle\right]\frac{dp'_s}{(1+e)p'_s} \tag{3}$$

Δe is the current value of the additional void ratio for loading along general stress paths, which can be defined by $\Delta e = e - e^*$. The sign function <> is necessary for the term Δe in Eq. (3) to ensure that the additional void ratio is nonnegative. The following equation defines the simple form of the sign function of Δe

$$\langle \Delta e \rangle = \begin{cases} \Delta e \text{ if } \Delta e \geq 0 \\ 0 \text{ if } \Delta e < 0 \end{cases} \tag{4}$$

The elastic deformation is presented in the first term of

Eq. (3), e.g.,

$$d\varepsilon_v^e = \frac{\kappa^*}{1+e}\left(\frac{dp'}{p'}\right) \tag{5}$$

The plastic strain part can be illustrated in the second term of Eq. (3) as

$$d\varepsilon^p_{v,\text{virgin yielding}} = \left[\left(\lambda^* - \kappa^*\right) + b\langle\Delta e\rangle\right]\frac{dp'_s}{(1+e)\,p'_s} \tag{6}$$

where $d\varepsilon^p_{v(*)}$ is the plastic volumetric deformation for the reconstituted soil and $d\varepsilon^p_{v(\Delta e)}$ is the plastic volumetric deformation due to the effect of soil structure. These are represented in the following equations

$$d\varepsilon^p_{v(*)} = \left(\lambda^* - \kappa^*\right)\frac{dp'_s}{(1+e)\,p'_s}, \tag{7}$$

$$d\varepsilon^p_{v(\Delta e)} = b\langle\Delta e\rangle\frac{dp'_s}{(1+e)\,p'_s}. \tag{8}$$

The incremental void ratio, de, can be calculated as follows

$$de = \left(d\varepsilon_v^e + d\varepsilon_v^p\right)(1+e). \tag{9}$$

Substituting Eqs. (5) and (6) into Eq. (9) gives

$$de = \kappa^*\left(\frac{dp'}{p'}\right) + \left[(\lambda^* - \kappa^*) + b\langle\Delta e\rangle\right]\frac{dp'_s}{p'_s}. \tag{10}$$

The application of Eq. (10) is shown by simulating the isotropic compression of natural Bangkok clay in Fig. 2. The following values for the soil parameters are employed in the simulation: λ^*=0.256, e^*_{IC}=2.78, e_0=2.306, $p'_{y,i}$=90 kPa, and b=1. It is seen that a nonsmooth continuity occurs between the elastic and plastic range. This is a deficiency in Liu and Carter's model due to the assumption of an elastic region before virgin yielding. This problem is solved in this study by incorporating the subyielding concept.

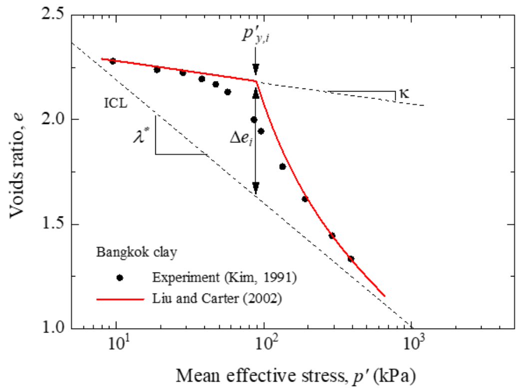

Fig. 2 Compression of Bangkok clay simulated by Liu and Carter's equation

3. Volumetric deformation during subyielding

3.1 Hypothesis and mathematical formulation

The occurrence of plastic deformation for loading before yielding is called "subyielding". The subyielding behavior of structured soils is studied. The structural yielding stress, p'_s, is defined as the boundary for the virgin yielding behavior. Subyielding occurs when $p'<p'_s$. The current state is denoted as p'_c, and its value varies with loading. Both hardening and destructuring are due to the plastic volumetric deformation associated with the current stress level (Liu and Carter 2003, Liu *et al.* 2006, Carter and Liu 2005).

Plastic volumetric deformation during subyielding is proposed based on experimental observation and with consideration of the following features of soil behavior.

• Smooth continuity exists when the soil behavior transfers from subyielding to virgin yielding.

• At the exact point when the stress path changes direction and soil behavior changes from virgin yielding to inside the virgin yielding boundary, there is no plastic deformation, $d\varepsilon^p_v$ =0.

The plastic deformation during subyielding is proposed based on the original form of plastic volumetric strain for structured soil (Eq. 6) with additional invariant parameters as follows

$$d\varepsilon^p_{v,\text{subyielding}} = \frac{\left(d\varepsilon^p_{v(*)} + \alpha^2 d\varepsilon^p_{v(\Delta e)}\right)}{\left[1 + (1-\alpha)\left(\lambda^*/\kappa^*\right)\right]}, \tag{11}$$

where α is an invariant parameter representing the stress history effect due to kinematic hardening on the plastic deformation of the soil. A simple scalar expression for α is suggested as

$$\alpha = \begin{cases} \left(\dfrac{p'_c - p'_{c,his}}{p'_s - p'_{c,his}}\right)^2 & \text{if } dp'_c \ge 0 \\[2ex] \left(1 - \dfrac{p'_c}{p'_s}\right)^2 & \text{if } dp'_c < 0 \end{cases}, \tag{12}$$

in which $p'_{c,his}$ is the value of the stress at which soil changes from unloading to loading, and p'_c is the current stress state. At the moment when soil yielding and dp'_c>0, virgin yielding commences.

By substituting Eqs. (7) and (8) into (11), the following general equation is obtained

$$d\varepsilon^p_{v,\text{subyielding}} = \frac{\left(\lambda^* - \kappa^*\right)dp'_c + \alpha^2 b\langle\Delta e\rangle\left|dp'_c\right|}{(1+e)\left[1 + (1-\alpha)\left(\lambda^*/\kappa^*\right)\right]p'_s}. \tag{13}$$

dp'_s is replaced by the dp'_c for representing the change in the size of loading surface. Because of the nature of soil structure, plastic deformation due to destructuring is irrecoverable by repeated loading. Δe is always positive. Thus, an absolute sign is introduced for the plastic deformation associated with destructuring.

Substituting Eqs. (5) and (13) into Eq. (9), the incremental void ratio, de, during isotropic compression for the subyielding range is expressed as follows

$$de = \kappa^*\left(\frac{dp'_c}{p'}\right) + \frac{\left(\lambda^* - \kappa^*\right)dp'_c + \alpha^2 b\langle \Delta e\rangle \left|dp'_c\right|}{\left[1+(1-\alpha)\left(\lambda^*/\kappa^*\right)\right]p'_s} \quad (14)$$

3.2 Influence of λ^*/κ^* on subyielding behavior

The invariant parameter, λ^*/κ^*, influences the subyielding deformation in Eq. (14). In practice, λ^*/κ^* varies between 2 to 30, and is a unique value based on the soil type. The influence of the compression ratio, λ^*/κ^*, between the plastic and elastic compression line on the subyielding behavior is investigated by the compression line of three natural clays as shown in Fig. 3. The Mattagami mines, Leda and Pisa clays have different values of λ^*/κ^*, and those are 21, 13.8 and 5.8, respectively. The transition between elastic to plastic deformation of structured clays is influenced by destructuring, which is dependent on the compression characteristics. A high destructuring rate during a preyield state is observed for soils with lower values of λ^*/κ^*.

The parametric study on λ^*/κ^* is performed for illustrating the performance of Eq. (14). The following values of soil parameters for compression modeling are employed in the parametric study: λ^*=0.256, e^*_{IC}=2.78, e_0=2.306, $p'_{y,i}$=90 kPa, and b=1. The simulations of the compression curves of clays under various values of λ^*/κ^* are shown in Fig. 4. The λ^*/κ^* values were varied over a range of 3.2 to 12.8. For high values of λ^*/κ^*, the soils behave stiffly and elastically. In the case where λ^*/κ^*< 12.8, it seems that the soil structure has been destroyed at the early stages of loading. The compression line slopes down to the yielding point while the slope of the compression line varies with the λ^*/κ^* ratio. The different destructuring of soil structure can be interpreted well by the invariant parameter, λ^*/κ^*, as proposed in Eq. (14).

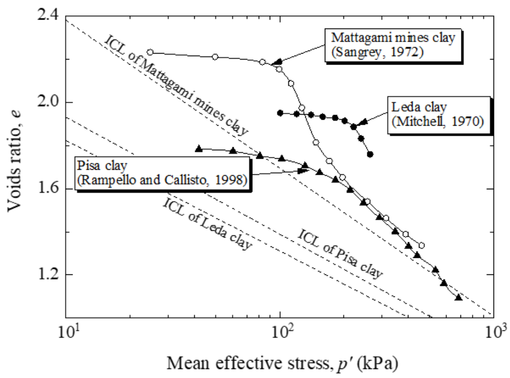

Fig. 3 Influence of λ^*/κ^* on the transition between subyielding and virgin yielding behavior

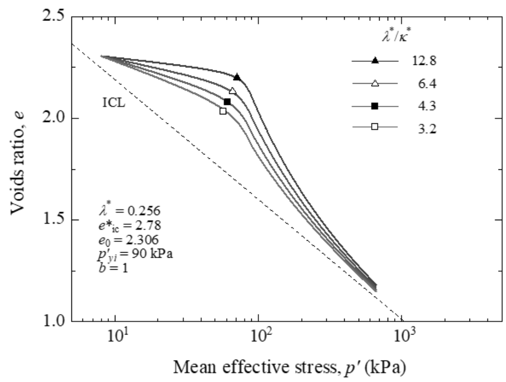

Fig. 4 Simulation of isotropic compression behavior of clays under various λ^*/κ^* values

Table 1 Model parameters for reconstituted kaolin

Parameter	λ^*	e^*_{IC}	κ^*	p'_0
Value	0.30	3.07	0.01	500

Table 2 Model parameters for structured clays

No.	Soil type	λ^*	e^*_{IC}	κ^*	$p'_{y,i}$	Δe_i	b
1	Mexico city clay	1.589	14.40	0.092	100	4.20	1.40
2	Mattagami mines clay	0.297	3.20	0.014	115	0.51	1.80
3	Pappadai clay	0.206	3.19	0.012	2,000	0.28	0.05
4	Bothkennar clay	0.273	2.42	0.018	60	0.64	0.20
5	Leda clay	0.222	2.33	0.016	230	0.81	0.60
6	Fort William Clay	0.123	1.26	0.020	350	1.60	0.40
7	Pisa clay	0.235	2.47	0.040	160	0.40	0.40
8	Bangkok clay	0.256	2.78	0.045	90	0.40	1.00
9	Osaka clay	0.147	1.92	0.030	90	0.60	0.30
10	Corinth marl	0.025	0.67	0.009	4,500	0.088	0.70

3.3 Performance of the improved compression model

The compression test results for eleven natural soils are assessed in order to verify the proposed work. All results are from isotropic compression tests obtained from the available literature. The physical parameters determined from ICL and SCL are listed in Tables 1 and 2 for reconstituted and naturally structured clays, respectively. The intrinsic parameters denoted by an asterisk are determined by curve fitting the isotropic compression line of the remolded sample (Liu and Carter 1999). The simulated compression curves have been calculated using Eq. (14).

The reconstituted kaolin test data, reported by Sivakumar *et al.* (2002) with an initial void ratio of approximately 1.16, are simulated by the subyielding concept without any effect of soil structure (Δe=0), as shown in Fig. 5. Solid symbols mark the selected results from the simulation. The tested results are presented as a solid line. For the reconstituted sample, λ^*/κ^* is greater than 33. The simulation result shows a good representation of both pre- and postyielding. A smooth compression curve (e−$\ln p'$) for both pre- and postyielding is observed. The

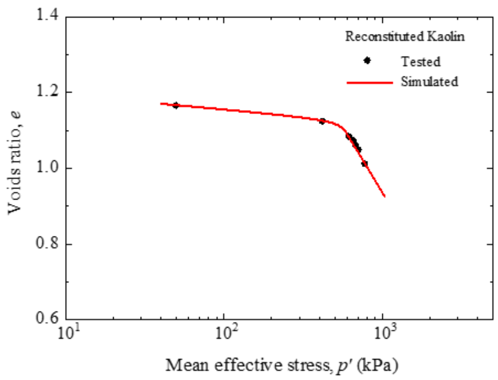

Fig. 5 Compression behavior of reconstituted kaolin

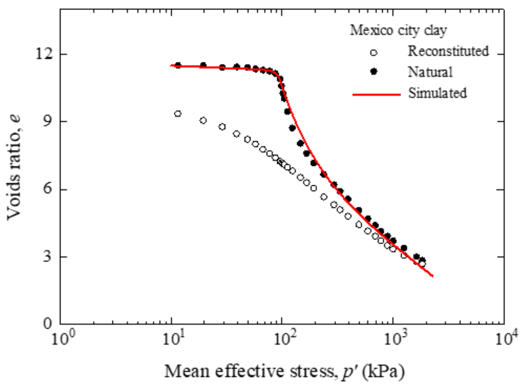

(a)

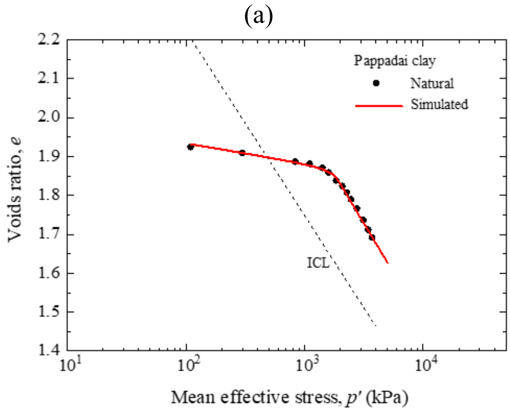

(b)

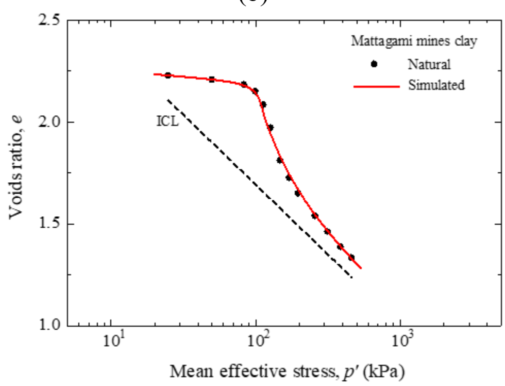

(c)

Fig. 6 Compression behavior of the Mexico city, Pappadai and Mattagami mines clays

proposed model can be used reliably in the efficient computation of reconstituted clay using only three

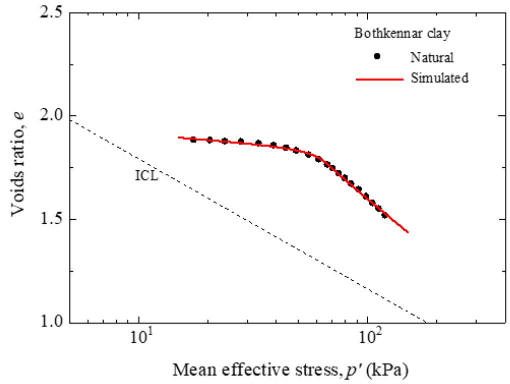

(a)

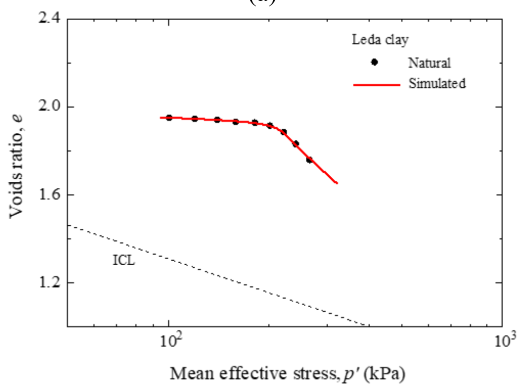

(b)

Fig. 7 Compression behavior of the Bothkennar and Leda clays

parameters (λ^*, e^*_{IC}, and κ^*) because the initial yielding stress, $p'_{y,i}$, of the soil is known.

The simulations of natural clays have been classified into three groups. The first group includes three different natural clays, with λ^*/κ^* varying from 17 to 33. Those are the Mexico City, Pappadai, and Mattagami mines clays. The comparisons between experiment and simulation are represented in Figs. 6(a) to 6(c). The Mexico City clay data were reported by Terzaghi (1953), and this clay is a very soft natural soil with a very high initial void ratio of 11.6. Cotecchia and Chandler (2000) have reported the test data for structured Pappadai clay. The soil is a very hard soil with, $p'_{y,i}$=2000kPa. The soft and sensitive Mattagami mines clay was reported by Sangrey (1972), with an initial void ratio of 2.23. The apparent slopes of the elastic and plastic compression lines of these three natural clays are quite different (high values of λ^*/κ^*).

The second group of test data includes natural clays with λ^*/κ^* varying from 9 to 16; they are the Bothkennar and Leda clays. The simulations for these clays are shown in Figs. 7(a) and 7(b), respectively. The high-compressibility Bothkennar clay was reported by Smith (1992). The initial void ratio of this clay is 1.88, which is a typical value for structured clays. The test pressure used ranged from 15 kPa to 120 kPa, and the reduction in void ratio was 0.36. The other clay named "Leda" is from Canada and was tested by Mitchell (1970). During the loading of the Leda clay from p'=100 kPa to 260 kPa, the void ratio decreased from 1.95

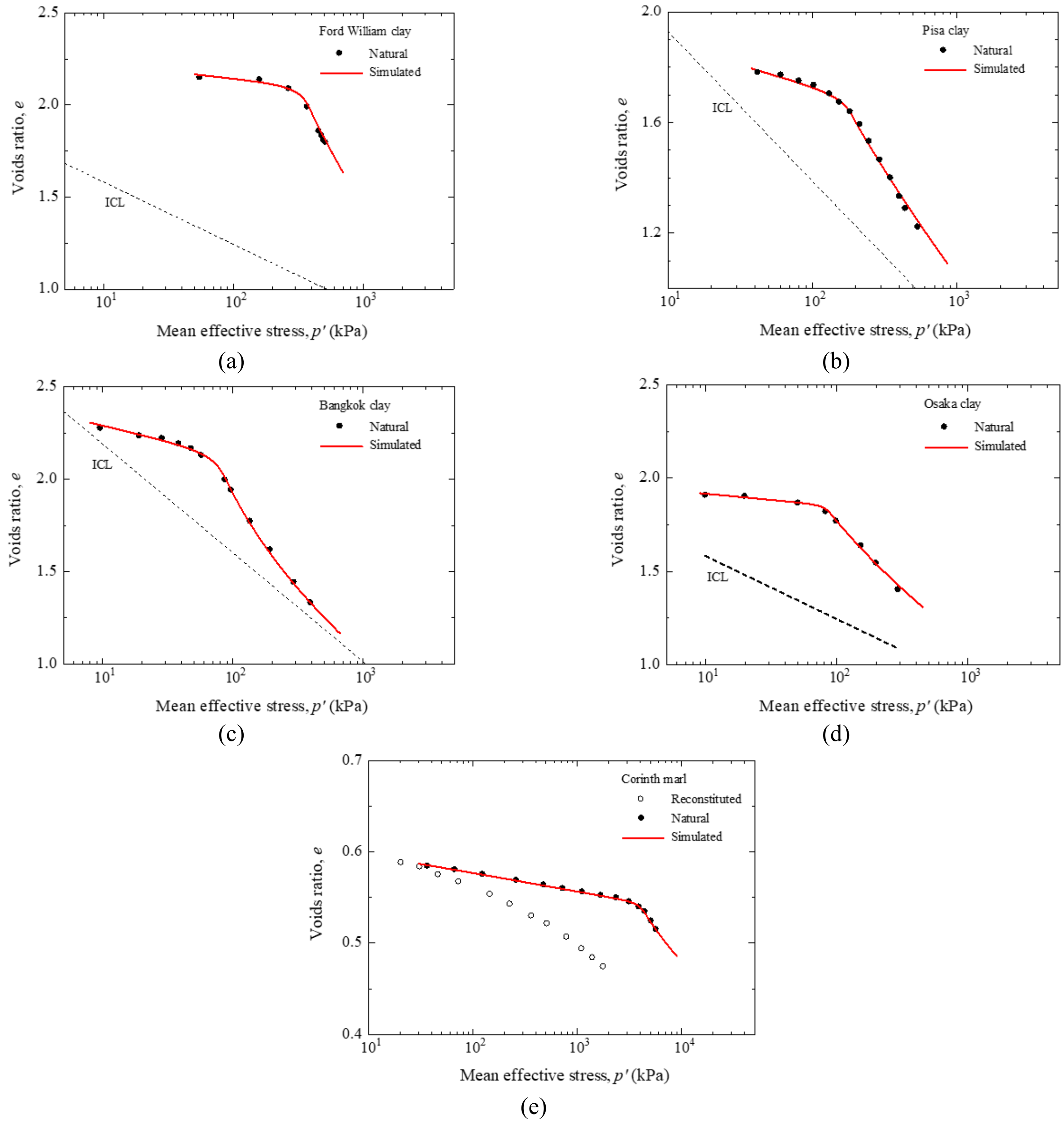

Fig. 8 Compression behavior of the Fort William, Pisa, Bangkok, Osaka clays and the Corinth marl

to 1.76.

The last group of test data consists of natural clays with λ^*/κ^* less than 7. Five different types of soil were considered. The first is a sensitive clay from the Thunder Bay area, Canada, known as the Fort William clay, which was reported by Eigenbrod and Burak (1991). The initial void ratio was 2.15, and the pressure ranged from 50 kPa to 550 kPa. The second is the compression test data of soft Pisa clay, reported by Rampello and Callisto (1998). Isotropic compression was performed with a high-quality sample at an initial void ratio of 1.78, with pressure ranging from 40 kPa to 680 kPa. The third was the natural, soft Bangkok clay, tested by Kim (1991) with a void ratio varying from 1.23 to 2.28. The fourth was the natural Osaka clay from Japan, tested by Adachi *et al.* (1995) with a void ratio varying from 1.91 to 1.40. The last clay was the structured stiff Corinth marl. The compression behavior of Corinth marl was reported by Anagnostopoulos *et al.* (1991). It had an initial void ratio of 0.59 and pressures ranging from 40 kPa to 5,600 kPa. The comparisons between the test data and the simulations are shown in Figs. 8(a)-8(e).

The ICL of the reconstituted samples has been given as a reference for all simulations. The additional void ratio, Δe, is the key parameter for modeling the structural compression line of clay in this study. The compression ratio, λ^*/κ^*, is an intrinsic property of a given soil, which is determined directly from the compression test of the soil in the reconstituted state. These parameters are included in the proposed Eqs. (13) and (14). The highly compressible behavior of different natural clays can be captured by the subyielding concept with the destructuring index value, b. When the stress state is far from the yield surface, the destructuring due to the compression path is small. This behavior controls by utilizing the α. When virgin yielding starts, $\alpha= 1$ and dp'_c is replaced by dp'_s, such that Eqs. (6) and (13) are the same. Virgin yielding occurs and the destructuring index, *b,* controls the compression behavior. As shown in Figs. 6 to 8, the volumetric deformations during isotropic compression of the soft to very stiff natural clays are simulated well by the proposed equation. A single theoretical equation can capture the sharp transition between the elastic and plastic compression of the three natural clays (*vide* Fig. 6). Overall, the compressional behaviors of ten different structured clays are simulated well by the proposed work, especially the elastic-plastic transition.

4. Shear behavior during subyielding

4.1 Surfaces in q-p' space

The SCC model is employed here for demonstrating the applicability of the proposed subyielding equations for the shearing behavior of structured soils, and details of the SCC framework can be found in published papers (Liu and Carter 2002, Carter and Liu 2005). The structural yield surface for clays is an elliptical shape, with the aspect ratio being the critical state strength, M^*. Thus

$$q^2 - M^{*2} p'\left(p'_s - p'\right) = 0 \tag{15}$$

p'_s is the size of the structural yield surface, which is the yield stress on the isotropic compression line. p'_s can be derived from the value of the stress state on the surface, i.e.,

$$p'_s = p'\left(M^{*2} + \eta^2\right) / M^{*2} \tag{16}$$

where η is the stress ratio (q/p').

The materials modeling of elastoplastic deformation has been developed based on two-surface theory (i.e., Dafalias and Popov 1975, Hashiguchi 1980). This theory is adopted in the proposed work. Fig. 9 presents the two surfaces concerned above; these are the structural yield and subyield surfaces.

Only changes in the sizes of the subyield and yield surfaces because of soil structure changes are considered while the effects of anisotropy are not examined in this work. An elliptical yield surface in the q-p' space is also assumed for structured clays with an aspect ratio of M^*. The size of the structural yield surface, p'_s, is the nonzero value of p' where the ellipse intersects the p' axis. Similarly, the subyield surface is also assumed to be elliptical and with the same aspect ratio, M^*. The formulation of the structural yield and the subyield surfaces is the same as in Eq. (15). The size of the subyield surface, p'_c is defined by a value which is determined entirely by the current stress state.

4.2 Plastic volumetric strain during shear

The total volume of the sample is constant in undrained shear conditions. Therefore, the elastic and plastic

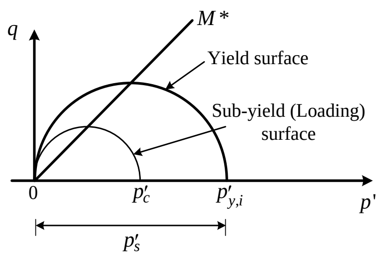

Fig. 9 Subyield and yield surfaces in q-p' space after Liu and Carter (2003)

volumetric strains must be both equal and opposite in sign, which results in zero volumetric deformation. During the virgin yielding, the magnitudes of the elastic and plastic volumetric strain increments are obtained from Eqs. (5) and (6). The plastic volumetric strain for the subyielding has been presented for isotropic compression loading following the Eq. (13). For the shearing mechanism, the plastic volumetric strain is dependent on both the change in the size of the subyield surface (dp'_c) and the magnitude of the current shear stress (Liu and Carter 2003, Suebsuk *et al.* 2011). Therefore, the following modification to Eq. (13) is made with the effect of destructuring along the stress path by an invariant parameter, $1-\frac{\eta}{M^*}$, as follows

$$d\varepsilon^p_{v,\text{subyielding}} = \left(1-\frac{\eta}{M^*}\right)\frac{\left(\lambda^*-\kappa^*\right)dp'_c + \alpha^2 b\langle\Delta e\rangle\left|dp'_c\right|}{(1+e)\left[1+(1-\alpha)\left(\lambda^*/\kappa\right)\right]p'_s} \tag{17}$$

The additional void ratio, Δe, varied depending on the variation of stress ratio, η, under loading or unloading is known as a destructuring process. This process has influenced the stress path represented by the parameter Δe in the second term of Eq. (17).

It can be seen from Eq. (17) that for the isotropic compression, $\eta=0$, that the plastic volumetric strain in Eq. (13) has recovered. Because of the modification made to Eq. (17), the plastic volumetric strain in the preyield state for structured clay is a nonzero value which depends on the destructuring and stress path.

The stress path of soils under undrained shear conditions is directly dependent on the plastic volumetric strain. The total volumetric strain is kept at zero due to the constant volume of soil during the undrained condition. Based on the elastoplastic concept, ε_v^e is equal to the negative of ε_v^p. The stress path can be calculated from the increment of shear stress, dq, and from the mean effective stress, dp', which is defined by rearrangement of Eq. (5) as follows

$$dp' = \frac{-d\varepsilon^p_v p'(1+e)}{\kappa} \tag{18}$$

Substituting Eq. (17) into Eq. (18), the increment of the mean effective stress during preyielding is obtained as follows

$$dp' = \left(\frac{\eta - M^*}{M^*}\right)\frac{\left(\lambda^*-\kappa^*\right)dp'_c + \alpha^2 b\langle\Delta e\rangle\left|dp'_c\right|}{\left[1+(1-\alpha)\left(\lambda^*/\kappa^*\right)\right]\kappa p'_s}p' \tag{19}$$

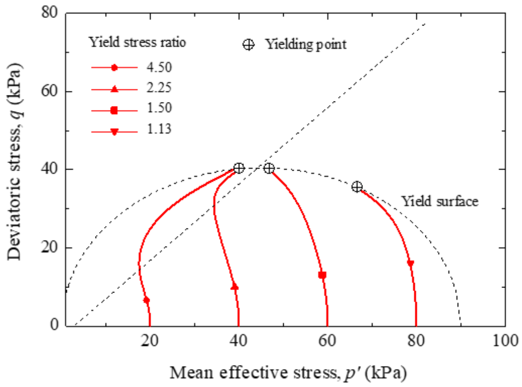

Fig. 10 Simulation of the undrained stress path during shear of structured clays under various YSR values

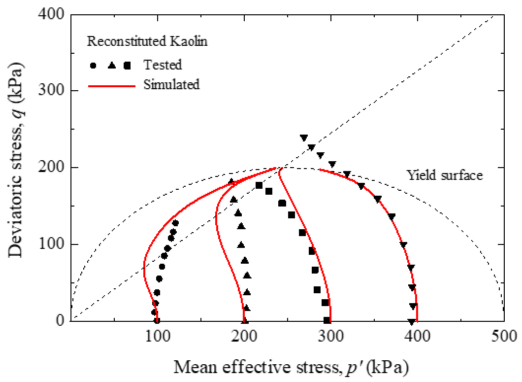

Fig. 11 Effective stress path of reconstituted kaolin

In summary, structured clay during undrained shearing is modeled as an isotropic hardening and destructuring material. The subyielding and virgin yielding behaviors are included in the formulation. The expansion of the subyield surface is due to the current stress and destructuring.

The values of soil parameters (e.g., λ^*, κ^*, e^*_{IC}, $p'_{y,i}$, and b) are reasonably calibrated from the isotropic compression tests previously described. M^* is required for Eqs. (17) and (19) for predicting the undrained stress path. It was determined from the slope of the critical state line (CSL) in q-p' space. The stress state has affected the stress path during preyielding via an invariant stress history, α. The simulation shown in Fig. 10 demonstrates the effect of the stress state on the plastic strain vector influenced on the undrained stress path during preyielding. The soil parameters used in these parametric studies of soft clays were: λ^*=0.256, κ^*=0.045, e^*_{IC}=2.78, e_0=2.306, $p'_{y,i}$=90 kPa, b=1, and M^*=0.9. Four different values of preshear effective stress were assumed, which varied from 20 kPa to 80 kPa. In each simulation, the soil had been isotropically consolidated to the preshear effective stress, and then experienced undrained shearing under compression loading. The stress path for lightly overconsolidated samples (yield stress ratio, YSR > 2) rises almost vertically towards the yield surface before moving towards the critical state. For the stress path of heavily overconsolidated samples (YSR < 2), they rise to the left-hand pass through the CSL and then move along close to the CSL and fail at the critical strength. The increasing stress ratio affects the change in the mean effective stress during shear by the term $1-\dfrac{\eta}{M^*}$ in Eq. (17).

4.3 Performance of the proposed model during undrained shear

The shearing behaviors of the reconstituted kaolin as well as six natural clays, e.g., Pisa clay, Osaka clay, Leda clay, Fort William clay, Pappadai clay, and Corinth marl, have been considered. The intrinsic and structured parameters were obtained using isotropic compression tests. The validity of the proposed model during shear was evaluated by drawing comparisons between the undrained triaxial compression test data and model simulations.

4.3.1 Reconstituted clay

The first group consists of results from four shearing tests on the reconstituted kaolin, reported by Sivakumar *et al.* (2002). The intrinsic parameters of reconstituted kaolin are listed in Table 1. The value of M^* for the reconstituted kaolin was reported as 0.8. Comparisons between simulation and experimental results of shear behavior are presented in Fig. 11. It may be noted that the intrinsic soil parameter determined from the compression test and M^* from the shearing test can be used to simulate the undrained stress path of clays in the reconstituted state under various preshear effective stresses.

4.3.2 Natural soft clays

The results of experimental work carried out on the natural Pisa clay (Rampello and Callisto 1998), natural Osaka clay (Adachi *et al.* 1995), natural Leda clay (Mitchell 1970) and the varved Fort William clay (Eigenbrod and Burak 1991) have been compared with the model simulations. Table 2 represents the intrinsic and structural soil parameters. The YSR varied with the preshear effective stress, ranging from the lightly overconsolidated clays to the heavily overconsolidated ones. The M^* value of the natural Pisa clay under undrained triaxial compression was observed as 1.2. The comparisons between the test and simulated data have been illustrated in a normalization space by an equivalent mean effective stress, p'_e, as shown in Fig. 12(a). According to the proposed volumetric deformation (Eq. 17), the behavior of the natural soft Pisa clay in a heavily overconsolidated state (YSR < 2) can be captured quite well with variation in the mean effective stress along with the loading ($dp'\neq0$).

The other natural soft clay from Osaka, Japan, was used in the shear validation. The λ^*/κ^* obtained from the intrinsic compression test is 4.9. M^* was determined from the data of the shearing tests as 1.70. The comparisons between the test and theoretical simulated data for the soil in different stress states are shown in Fig. 12(b). It is seen that the shear behaviors of Osaka clay have been simulated satisfactorily by the proposed model.

Three undrained shear tests on natural Leda clays, performed by Mitchell (1970), were also used to validate the model. The initial state of structured Leda clay is defined by $p'_{y,i}$=230 kPa, and the preshear effective stress

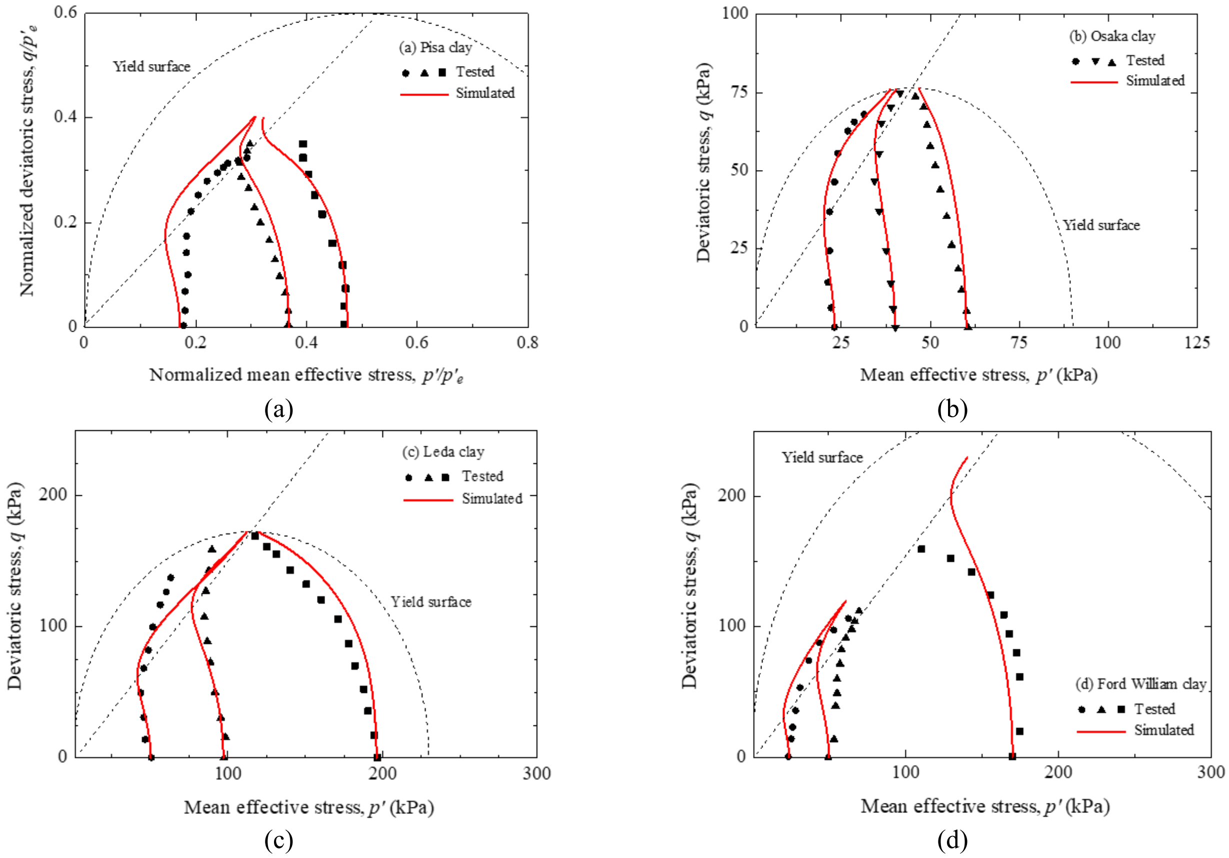

Fig. 12 Effective stress paths for the Pisa, Osaka, Leda, and Fort William clays

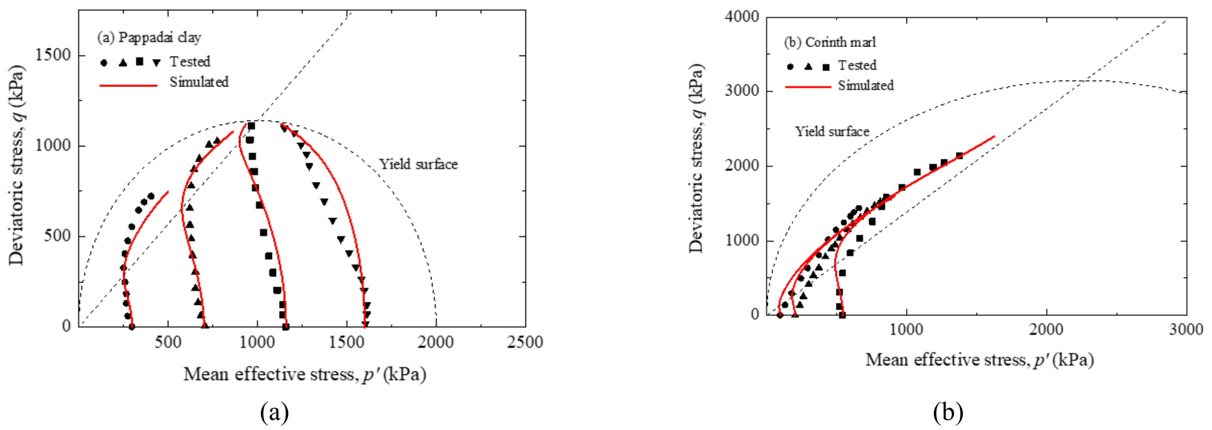

Fig. 13 Effective stress paths of the Pappadai clay and Corinth marl

varied from 50 kPa to 200 kPa. A comparison between the test and simulated data is shown in Fig. 12(c). The proposed equation provides a reasonable description of the undrained stress path for natural Leda clays.

The test data of a sensitive clay from the Thunder Bay area, Canada, previously known as Fort William clay, were also considered in this study. For the three shear tests, the initial stress state of the soil is a structural yield surface. The initial state was defined by $p'_{y,i}$=350 kPa. The soil samples for these tests were the overconsolidated structured soils. In this simulation, the M^* of 1.54 was calibrated from the three shear tests. A comparison between the test and simulated data is shown in Fig. 12(d). All samples of the Fort William clay were on the dry side of CSL with σ'_c= 25, 50 and 170 kPa; the increment of the mean effective stress dp' had a negative sign from the early stage of loading. However, the sign convention is reversed when $\eta>M^*$. Overall, it is seen that the proposed volumetric strain model provides a reasonably reliable prediction for the shear behavior of sensitive, soft clays.

4.3.3 Natural stiff clay

The behaviors of stiff Pappadai clay under conventional undrained triaxial tests were predicted by using the soil parameters listed in Table 2. Four shear tests were considered, with the preshear mean effective stress varying from 300 to 1,600 kPa. A comparison between the test and simulated results of the four shear tests is shown in Fig. 13(a). The structural yield surface defined with $p'_{y,i}$=2000 kPa and M^{*}=1.14 is illustrated. The undrained effective stress paths located within the structural yield surface have been captured with the model simulation.

The results of the undrained triaxial compression test of a natural Corinth marl reported by Ananostopoulos *et al.* (1991) are compared with the proposed model. The simulation using soil parameters is listed in Table 2, while the heavily overconsolidated behavior of the natural Corinth marl is shown in Fig. 13(b). The confining pressures were kept constant at 97, 202, and 545 kPa, respectively. For all three shearing tests, the initial stress states are inside the structural yield surface. Although the structured stiff soils have a strong soil structure, which cannot be degraded entirely under compression loading and unloading, the complex destructuring process of these soils during shear can be modeled by the proposed subyield concept with only six parameters.

5. Conclusions

In this article, a volumetric deformation model describing the subyielding and virgin yielding responses of structured clays is proposed. The demonstration of the model's ability to simulate the compression and shear responses of natural clays under the different soil structures (viz. reconstituted, sensitive and stiff clays) is presented. Overall, preyield and postyield behaviors of the soils can be reasonably interpreted over the influence of various types of soil structures. The modeling of clay behavior in reconstituted, and structured states can be unified into one consistent theoretical framework. The SCC model incorporating the subyielding concept and its mathematical formulation are presented. The model parameters can be calibrated reasonably from conventional compression and shear tests. The proposed model has the potential to solve the geological and geotechnical engineering problems involving various types of structured clays.

Acknowledgments

The first author would like to acknowledge the financial support provided by the Rajamangala University of Technology Isan; Office of the Higher Education Commission, Thailand; and the Thailand Research Fund (TRF) under contract MRG5580056. The second author is grateful for the financial support from the Thailand Research Fund under the TRF Senior Research Scholar Program.

References

Adachi, T., Oka, F., Hirata, T., Hashimoto, T., Nagaya, J., Mimura, M. and Pradhan, T.B.S. (1995), "Stress-strain behavior and yielding characteristics of eastern Osaka clay", *Soils Found.*, **35**(3), 1-13. https://doi.org/10.3208/sandf.35.1.

Anagnostopoulos, A.G., Kalteziotis, N. and Tsiambaos, G.K. (1991), "Geotechnical properties of the Carinth Canal marls", *Geotech. Geol. Eng.*, **9**(1), 1-26. https://doi.org/10.1007/BF00880981.

Baudet, B. and Stallebrass, S. (2004), "A constitutive model for structured clays", *Geotechnique*, **54**(4), 269-278. https://doi.org/10.1680/geot.2004.54.4.269.

Burland, J.B. (1990), "On the compressibility and shear strength of natural soils", *Geotechnique*, **40**(3), 329-378. https://doi.org/10.1680/geot.1990.40.3.329.

Callisto, L. and Rampello, S. (2004), "An interpretation of structural degradation for three natural clays", *Can. Geotech. J.*, **41**(3), 392-407. https://doi.org/10.1139/t03-099.

Carter, J.P. and Liu, M.D. (2005), "Review of the Structure Cam Clay model. soil constitutive models: evaluation, selection, and calibration", *ASCE Geotech. Special Publ.*, **128**, 99-132.

Carter, J.P., Airey, D.W. and Fahey, M. (2000), *A Review of Laboratory Testing of Calcareous Soils*, in *Engineering for Calcareous Sediments*, 401-431.

Chai, J.C., Shen, S.L., Zhu, H.H. and Zhnag, X.L. (2004), "Land subsidence due to groundwater drawdown in Shanghai", *Geotechnique*, **54**(2), 143-147.

Chen, B., Xu, Q. and Sun, D. (2014), "An elastoplastic model for structured clays", *Geomech. Eng.*, **7**(2), 213-231. https://doi.org/10.12989/gae.2014.7.2.213.

Cheng, X. and Wang, J. (2016), "An elastoplastic bounding surface model for the cyclic undrained behavior of saturated soft clays", *Geomech. Eng.*, **11**(3), 325-343. https://doi.org/10.12989/gae.2016.11.3.325.

Cotecchia, F. and Chandler, R.J. (2000), "A general framework for the mechanical behaviour of clays", *Geotechnique*, **50**(4), 431-447.

Dafalias, Y.F. and Popov, E.P. (1975), "A model of non-linearly hardening materials for complex loading", *Acta Mechanica*, **21**(3), 173-192. https://doi.org/10.1007/BF01181053.

Eigenbrod, K.D. and Burak, J.B. (1991), "Effective stress paths and pore-pressure responses during undrained shear along the bedding planes of varved Fort William clay", *Can. Geotech. J.*, **28**(6), 804-811. https://doi.org/10.1139/t91-097.

Gajo, A. and Muir Wood, D. (2001), "A new approach to anisotropic, bounding surface plasticity: general formulation and simulations of natural and reconstituted clay behavior", *Int. J. Numer. Anal. Meth. Geomech.*, **25**(3), 207-241. https://doi.org/10.1002/nag.126.

Gens, A. and Nova, R. (1993), "Conceptual bases for constitutive model for bonded soil and weak rocks", *Proceedings of the International Symposium on Geotechnical Engineering of Hard Soil-Soft Rocks*, Athens, Greece, September.

Gylland, A., Long, M., Emdal, A. and Sandven, R. (2013), "Characterisation and engineering properties of Tiller clay", *Eng. Geol.*, **164**, 86-100. https://doi.org/10.1016/j.enggeo.2013.06.008.

Hashiguchi, K. (1980), "Constitutive equations of elastoplastic materials with elastic-plastic translation", *J. Appl. Mech.*, **47**, 266-272. https://doi.org/10.1115/1.3153653.

Herbstová, V. and Herle, I. (2009), "Structure transitions of clay fills in North-Western Bohemia", *Eng. Geol.*, **104**(3-4), 157-166.

Horpibulsuk, S., Shibuya, S., Fuenkajorn, K. and Katkan, W. (2007), "Assessment of engineering properties of Bangkok clay", *Can. Geotech. J.*, **44**(2), 173-187. https://doi.org/10.1139/t06-101.

Kavvadas, M. and Amorosi, A. (2000), "A constitutive model for structured soils", *Geotechnique*, **50**(3), 263-273. https://doi.org/10.1680/geot.2000.50.3.263.

Kim, S.R. (1991), "Stress-strain behaviour and strength characteristics of lightly overconsolidated clays", Ph.D. Dissertation, Asian Institute of Technology, Bangkok, Thailand.

Leroueil, S. and Vaughan, P.R. (1990), "The general and congruent effects of structure in natural soils and week rock", *Geotechnique*, **40**(3), 467-488. https://doi.org/10.1680/geot.1990.40.3.467.

Liu, M.D. and Carter, J.P. (1999), "Virgin compression of structured soils", *Geotechnique*, **49**(1), 43-57. https://doi.org/10.1680/geot.1999.49.1.43.

Liu, M.D. and Carter, J.P. (2000), "Modeling the destructuring of soils during virgin compression", *Geotechnique*, **50**(4), 479-483.

Liu, M.D. and Carter, J.P. (2002), "A structured Cam Clay model", *Can. Geotech. J.*, **39**(6), 1313-1332. https://doi.org/10.1139/t02-069.

Liu, M.D. and Carter, J.P. (2003), "Volumetric deformation of natural clays", *Int. J. Geomech.*, **3**(2), 236-252. https://doi.org/10.1061/(ASCE)1532-3641(2003)3:2(236).

Liu, M.D., Carter, J.P., Horpibulsuk, S and Liyanapathirana, D. (2006), "Modelling the behaviour of cemented clay", *Geotech. Special Publ.*, 65-72.

Locat, J. and Lefebvre, G. (1985), "The compressibility and sensitivity of an artificially sedimented clay soil: The Grande-Baleine marine clay, Quebec", *Mar. Geotechnol.*, **6**(1), 1-27.

Mitchell, R.J. (1970), "On the yielding and mechanical strength of Leda clays", *Can. Geotech. J.*, **7**(3), 297-312. https://doi.org/10.1139/t70-036.

Ouria, A. (2017), "Disturbed state concept–based constitutive model for structured soils", *Int. J. Geomech.*, **17**(7), 04017008. https://doi.org/10.1061/(ASCE)GM.1943-5622.0000883.

Park, D. (2016), "Rate of softening and sensitivity for weakly cemented sensitive clays", *Geomech. Eng.*, **10**(6), 827-836.

Rampello, S. and Callisto, L. (1998), "A study on the subsoil of the tower of Pisa based on results from standard and high-quality samples", *Can. Geotech. J.*, **35**(6), 1074-1092. https://doi.org/10.1139/t98-055.

Roscoe, K.H. and Burland, J.B. (1968), "On the generalised stress-strain behaviour of wet clay", *Eng. Plasticity*, 535-609.

Roscoe, K.H. and Schofield, A.N. (1963). "Mechanical behaviour of an idealised wet clay", *Proceedings of the European Conference on Soil Mechanics and Foundation Engineering*, Wiesbaden, Germany.

Rouainia, M. and Muir Wood, D. (2000), "A kinematic hardening constitutive model for natural clays with loss of structure", *Geotechnique*, **50**(2), 153-164. https://doi.org/10.1680/geot.2000.50.2.153.

Sangrey, D.A. (1972), "Naturally cemented sensitive soils", *Geotechnique*, **22**(1), 139-152. https://doi.org/10.1680/geot.1972.22.1.139.

Schmertmann, J.H. (1991), "The mechanical aging of soils", *J. Geotech. Eng.*, **117**(9), 1288-1330. https://doi.org/10.1061/(ASCE)0733-9410(1991)117:9(1288).

Schofield, A.N. and Wroth, C.P. (1968), *Critical State Soil Mechanics*, McGraw-Hill, London, U.K.

Shen, S.L. and Xu, Y.S. (2011), "Numerical evaluation of land subsidence induced by groundwater pumping in Shanghai", *Can. Geotech. J.*, **48**(9), 1378-1392. https://doi.org/10.1139/t11-049.

Shen, S.L., Ma, L., Xu, Y.S. and Yin, Z.Y. (2013), "Interpretation of increased deformation rate in aquifer IV due to groundwater pumping in Shanghai", *Can. Geotech. J.*, **50**(11), 1129-1142. https://doi.org/10.1139/cgj-2013-0042.

Sivakumar, V., Doran, I.G. and Graham, J. (2002), "Particle orientation and its influence on the mechanical behaviour of isotropically consolidated reconstituted clay", *Eng. Geol.*, **66**(3-4), 197-202. https://doi.org/10.1016/S0013-7952(02)00040-6.

Smith, P.R. (1992), "The behaviour of natural high compressibility clays with special reference to consolidation on soft ground", Ph.D. Thesis, University of London, London, U.K.

Suebsuk, J., Horpibulsuk, S. and Liu, M.D. (2011), "A critical state model for overconsolidated structured clay", *Comput. Geotech.*, **38**(5), 648-658. https://doi.org/10.1016/j.compgeo.2011.03.010.

Sun, D., Chen, L., Zhang, J. and Zhou, A. (2015), "Bifurcation analysis of over-consolidated clays in different stress paths and drainage conditions", *Geomech. Eng.*, **9**(5), 669-685. https://doi.org/10.12989/gae.2015.9.5.669

Terzaghi, K. (1953), "Fifty years of subsoil exploration", *Proceedings of the 3rd International Conference on Soil Mechanics and Foundation Engineering*, Switzerland, August.

Yao, Y.P. and Zhou, A.N. (2013), "Non-isothermal unified hardening model: A thermo-elastoplastic model for clay", *Geotechnique*, **63**(15), 1328-1345. http://dx.doi.org/10.1680/geot.13.P.035.

Yao, Y.P., Hou, W. and Zhou, A.N. (2009), "UH model: Three-dimensional unified hardening model for overconsolidated clays", *Geotechnique*, **59**(5), 451-469. https://doi.org/10.1680/geot.2007.00029.

Yao, Y.P., Sun, D.A. and Matsuoka, H. (2008), "A unified constitutive model for both clay and sand with hardening parameter independent on stress path", *Comput. Geotech.*, **35**(2), 210-222. https://doi.org/10.1016/j.compgeo.2007.04.003.

Zhang, H., Chen, Q., Chen, J. and Wang, J. (2017), "Application of a modified structural clay model considering anisotropy to embankment behavior", *Geomech. Eng.*, **13**(1), 79-97. https://doi.org/10.12989/gae.2017.13.1.079.

Zhu, E.Y. and Yao, Y.P. (2015), "Structured UH model for clays", *Transportation Geotech.* **3**, 68-79. https://doi.org/10.1016/j.trgeo.2015.03.003.

GC